

## Spin-wave dispersion in magnetostrictive Fe-Ga alloys: Inelastic neutron scattering measurements

J. L. Zarestky,<sup>1</sup> O. Moze,<sup>2</sup> J. W. Lynn,<sup>3</sup> Y. Chen,<sup>3,4</sup> T. A. Lograsso,<sup>5</sup> and D. L. Schlage<sup>1</sup><sup>1</sup>Ames Laboratory and Department of Physics and Astronomy, Iowa State University, Ames, Iowa 50011, USA<sup>2</sup>Dipartimento di Fisica, Università di Modena e Reggio Emilia, Modena 41100, Italy<sup>3</sup>NIST Center for Neutron Research, National Institute of Standards and Technology, Gaithersburg, Maryland 20899-8562, USA<sup>4</sup>Department of Materials Science and Engineering, University of Maryland, College Park, Maryland 20742, USA<sup>5</sup>Ames Laboratory, Materials and Engineering Physics Program, Iowa State University, Ames, Iowa 50011, USA

(Received 16 November 2006; published 12 February 2007)

Fe-Ga alloys of appropriate Ga concentration and heat treatment show a very large enhancement in the tetragonal magnetostriction over that of pure  $\alpha$ -Fe [ $\lambda_{100}(\text{Fe-Ga}) \sim 15\lambda_{100}(\text{Fe})$ ]. In order to gain further understanding of the extraordinary magnetoelastic characteristics of this system, the spin dynamics of two of these alloys,  $\text{Fe}_{1-x}\text{Ga}_x$  ( $x=0.160$  and  $0.225$ ), were studied using inelastic neutron scattering techniques. The correlation of the spin-wave dispersion curve with the lattice constant and atomic radii of solute is examined for this and other Fe alloys.

DOI: 10.1103/PhysRevB.75.052406

PACS number(s): 75.50.Bb, 75.80.+q, 78.70.Nx, 63.20.-e

## I. INTRODUCTION

Dilute solid solution magnetostrictive alloys of Fe continue to be the focus of fundamental experimental research because of their potential for application in devices such as sensors and transducers.<sup>1-3</sup> Much of this research is aimed at obtaining the microscopic description of the observed magnetostrictive behavior of these materials. Alloys of Fe with Al, Ga, and Be all show enhancement of the tetragonal magnetostriction coefficient,  $\lambda_{100}$ , which, in the case of Ga, is a factor of 15 over that of pure Fe. This enhancement is accompanied by a dramatic softening of the elastic constants, in particular,  $C' = \frac{1}{2}(C_{11} - C_{12})$ . Sound velocity measurements<sup>4-6</sup> found that  $C'$  decreases linearly with increasing Ga concentration and extrapolates to zero at around 28 at. % Ga.

Further insight to the extraordinary magnetoelastic behavior in this system was provided by inelastic neutron scattering measurements<sup>7</sup> on the Fe-Ga system, performed on a series of compositions ( $\text{Fe}_{1-x}\text{Ga}_x$ ,  $x=0.108, 0.133, 0.160, 0.225$ , and  $0.288$ ) that showed all branches soften with increased Ga concentration. Most notably, however, was that the  $T_2[110]$  branch (polarization in the  $[\bar{1}10]$  direction) softened dramatically by 50% over the composition range studied. The elastic constant  $C'$  is directly related to the slope of this branch at low  $q$ . A recent study<sup>8</sup> of the lattice dynamics of Fe-Be with 10 at. % showed a similar softening of the  $T_2[110]$  branch for that alloy. The spin wave dispersion was also measured in the Fe-Be experiments. In order to present a complete picture of the Fe-Ga system, we report here the results of spin-wave dispersion curve measurements on two compositions ( $x=0.160$  and  $0.225$ ) of  $\text{Fe}_{1-x}\text{Ga}_x$ .

## II. EXPERIMENT

The measurements were performed using the same 16.0 and 22.5 at. % Ga crystals used in the previous lattice dynamical study.<sup>7</sup> Sample preparation details can be found there. Those measurements determined that the 16.0 at. % sample was entirely of the disordered  $B2$  phase, while the

22.5 at. % sample contained an  $\sim 24\%$   $DO_3$  phase. Samples were mounted in an aluminum can under helium atmosphere and were cooled in a closed cycle helium refrigerator (CCHR). The sample was held at a base temperature of  $\sim 4.2$  K to reduce the background from multiphonon (and multimagnon) scattering.

The CCHR was mounted on the sample table of the BT-7 triple-axis neutron spectrometer of the NIST Center for Neutron Research. The instrument was operated, with only a few exceptions, in the constant energy transfer mode with a fixed final energy of 14.7 meV. Collimation was open-50'-40'-200' and a highly oriented pyrolytic graphite (HOPG) filter before the analyzer was used to reduce higher-order contaminations. Apertures before and after the sample position masked the incident and scattered beams to a size just over that of the sample. The sample was oriented with the  $(h, k, 0)$  plane of the crystal in the scattering plane of the instrument, that is, with a (001) vertical reciprocal lattice vector. All spin-wave neutron groups were measured from the  $[110]$  reciprocal lattice point and in both the transverse and longitudinal directions whenever possible. As a check, some scans were also made in the (100) direction from the  $[110]$ . No temperature dependence of the spin waves was measured, nor were detailed scans enabling intensity analysis taken.

## III. RESULTS AND DISCUSSION

Figure 1 shows some typical neutron groups for  $L[\xi\xi0]$  constant energy scans on  $\text{Fe}_{0.835}\text{Ga}_{0.165}$ . Scans were performed to obtain the dispersion to energies up to 60 meV and out to values of  $q \approx 0.8 \text{ \AA}^{-1}$  (the zone boundary is at  $q = 1.52 \text{ \AA}^{-1}$ ). The measured spin-wave dispersion curves for the two Fe-Ga sample compositions are shown in Fig. 2. For comparison purposes, the spin-wave dispersion curves (fitted curves) of  $\alpha$ -Fe (Refs. 9-12) and  $\text{Fe}_{0.9}\text{Be}_{0.1}$  (Ref. 8) are also shown in this figure. There is a notable softening of the spin-wave dispersion proceeding from  $\alpha$ -Fe to  $\text{Fe}_{0.9}\text{Be}_{0.1}$  to the two Fe-Ga compositions studied here.

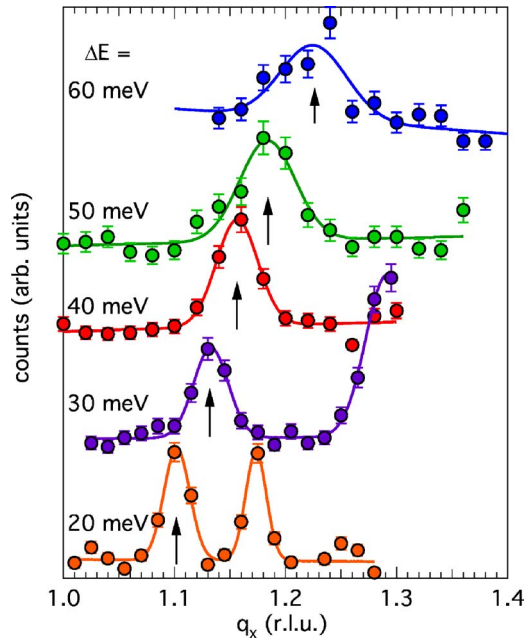


FIG. 1. (Color online) Neutron groups for  $L[\xi\xi 0]$  constant energy scans on  $\text{Fe}_{1-x}\text{Ga}_x$  ( $x=0.165$ ). The second peaks in the 20 and 30 meV scans are scattered from the  $L[\xi\xi 0]$  phonon.

For both Ga compositions, the agreement of spin-wave  $q$  values obtained at a particular energy transfer, between longitudinal and transverse scans, was very good and well within the experimental error. Results of scans in the (100)

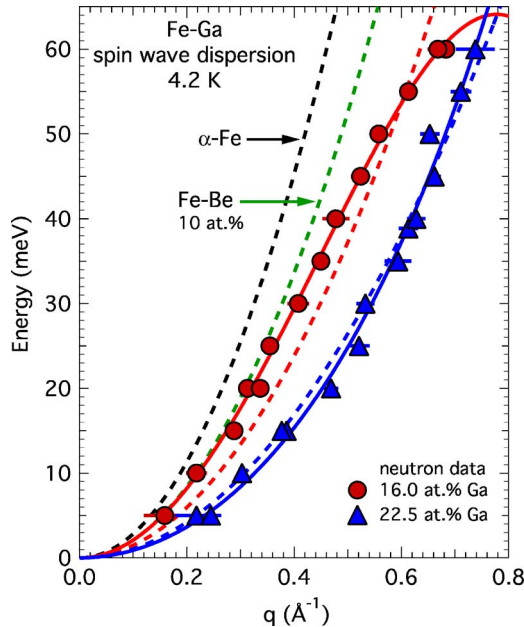


FIG. 2. (Color online) Neutron measured spin wave dispersion curves for two  $\text{Fe}_{1-x}\text{Ga}_x$  alloys,  $x=0.108$  (red, circles) and  $x=0.225$  (blue, triangles). Horizontal lines through points indicate errors in  $q$ . The dashed curves, in order of decreasing  $D$ , are quadratic fits for  $\alpha\text{-Fe}$  (Refs. 9–11) (black),  $\text{Fe}_{1-x}\text{Be}_x$  (Ref. 8) ( $x=0.10$  green), and  $\text{Fe}_{1-x}\text{Ga}_x$  ( $x=0.160$ , red and  $x=0.225$ , blue). The solid curves are the fourth order fits for the two Fe-Ga alloys (red and blue, respectively).

direction also agreed with those in the (110) direction to within the experimental error. This is consistent with an isotropic spin-wave dispersion relation for a ferromagnetic system. Also, no anomalous behavior that could be attributed to the interaction between phonons and magnons was observed. It should be noted, however, that the  $T_2[110]$  branch crosses the spin-wave dispersion curve at an energy below 2 meV and for  $q$  less than  $0.15 \text{ \AA}^{-1}$ , a region where elastic, phonon, and spin-wave scattering would all be observed and would make separation difficult, given the experimental conditions here.

Experimental spin-wave dispersion data have traditionally been analyzed in terms of the nearest-neighbor Heisenberg model. In this model, for modes along the high symmetry directions of the 3d metals and for small  $q$ , the spin-wave energy reduces<sup>9,10</sup> to

$$\hbar\omega = C + Dq^2(1 - \beta q^2 + \gamma q^4 - \dots).$$

In most cases, spin-wave dispersion data can be adequately described using the following simplified expression:

$$\hbar\omega = Dq^2(1 - \beta q^2).$$

Applying least-squares methods to these expressions, the constants  $D$  and  $\beta$  (and, when necessary,  $C$  and  $\gamma$ ) can be determined and compared with other materials.

The 22.5 at. % Ga data were analyzed using the above expressions, and a reasonable fit was obtained using only the  $Dq^2$  term. There was, however, an improvement in the fit by adding the fourth-order term, giving  $D=89.8 \pm 6.1 \text{ meV \AA}^2$  and  $\beta=-0.42 \pm 0.19 \text{ \AA}^2$ . Fitting the data using the constant and sixth-order terms showed only a slight improvement. The latter fit indicated a gap of  $1.42 \pm 2.83 \text{ meV}$ . For highly dispersive systems such as this, most of the experimental error is from the  $q$  dependence of the instrumental resolution.<sup>13</sup> At the elastic condition, for the configuration of BT7 used, the energy width of the resolution function was  $\sim 1.6 \text{ meV}$  and the  $q$  width was  $\sim 0.1 \text{ \AA}^{-1}$ . This and the large statistical error imply that no significance should be attributed to an energy gap of this size.

A satisfactory fit to the 16.0 at. % Ga data was not possible with only the quadratic term in  $q$ . Including the fourth-order term in  $q$  did improve this fit a great deal, giving values of  $D=211.9 \pm 3.3 \text{ meV \AA}^2$  and  $\beta=0.83 \pm 0.03 \text{ \AA}^2$ , but additional fits using the constant and sixth-order terms showed only a slight improvement, just as they did for the previous sample. The quadratic and fourth-order fits are shown in Fig. 2. A fit of the data for  $\hbar\omega < 55 \text{ meV}$  to  $Dq^2$  was also performed using only the quadratic term. The fit was much better than the corresponding fit for the full range of energies, but still not as good as the fourth-order fit, demonstrating that even the low-energy data clearly indicate a significant deviation from the simple quadratic dependence.

The values of  $D$  calculated for the two alloys of Fe-Ga are plotted as a function of Ga concentration in Fig. 3. The value for  $D$  of 16.0 at. % Ga is in reasonable agreement with the values of  $D$  found by Antonini and Stringfellow<sup>14</sup> using the small-angle neutron scattering technique. The values of  $D$  versus their respective alloy compositions for  $\alpha\text{-Fe}$  and other Fe alloys are also shown in this figure using the triple-axis,

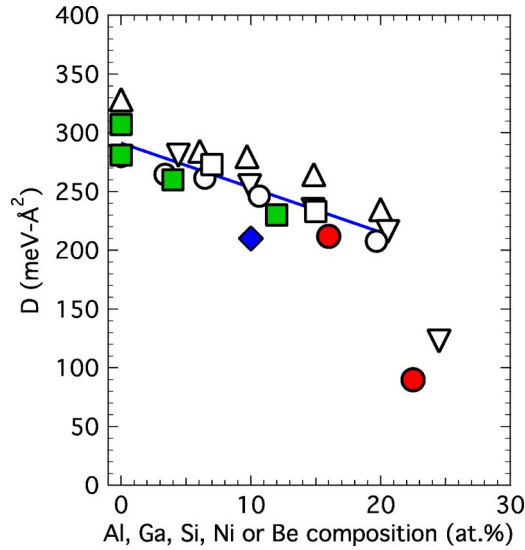


FIG. 3. (Color online) Values of the dispersion parameter  $D$  determined by triple-axis neutron scattering (filled symbols) for Fe-Ga alloys (this work) (red, circles),  $\alpha$ -Fe (Refs. 9–11) and Fe-Si alloys (Refs. 11 and 12) (green, squares), and Fe-Be (Ref. 8) (blue, diamond). Values of  $D$  determined by small-angle neutron scattering or the neutron diffraction and/or polarized method are shown as open symbols; Fe-Ga (Ref. 14) (circles), Fe-Al (Ref. 14) (inverted triangles), Fe-Si (Ref. 15) (squares), and Fe-Ni (Ref. 16) (triangles). The blue line is a linear fit to all data points for alloys with concentration  $\leq 20$  at. %.

small-angle, and polarized neutron diffraction techniques. (It should be noted that the data for Fe-Ni, Fe-Al, and Fe-Ga using the small-angle technique and the data for Fe-Ga reported here are for 0 K or low temperatures, while the remaining examples are room temperature data.) From this rough comparison, the behavior of  $D$  appears to be largely independent of the solute. However, there seems to be an approximately linear dependence on the solute concentration in the alloy, up to  $\sim 20$  at. %, as shown by the blue line in Fig. 3. Of course, above this concentration, conditions become favorable for the formation of the ordered  $DO_3$  structure.

In order to see if the behavior of  $D$  versus composition is related to the lattice size, we examined the lattice parameter  $a$  of these martensitic solid solution Fe alloys as a function of composition. There appears to be three distinctly different types of behavior of  $a$ , as seen in Fig. 4. The first is exemplified by Fe-Al and Fe-Ga alloys, where the lattice expands with increased solute and is indicated by the upper group or “branch” of lattice parameters in Fig. 4. The second group includes Fe-Si, Fe-Ni, and Fe-Co alloys, where there is little change in the lattice parameter from  $\alpha$ -Fe with increased solute and is seen as a flat branch of data points in Fig. 4. Fe-Be alloys represent the third type of behavior with the lattice decreasing in size with increasing Be content. This branch behavior for  $a$  versus composition, however, does not indicate any correlation between lattice parameter  $a$  and  $D$ , suggesting that the spin-wave dispersion relation originates from the electron correlations via the band structure (as it does in Fe and Ni).

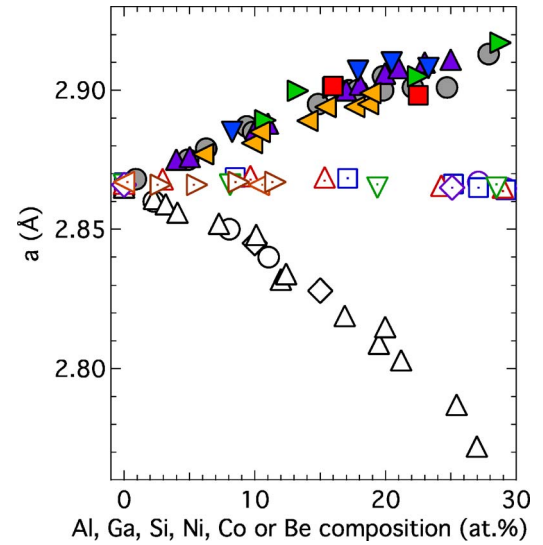


FIG. 4. (Color online) Lattice parameters of solid solution alloys vs composition (at. %) for Fe-Ga (Refs. 17–20) and Fe-Al (Ref. 20) (filled symbols, various colors), Fe-Si (Refs. 21–23), Fe-Ni (Refs. 24 and 25), and Fe-Co (Ref. 26) (open symbols with points, various colors), and Fe-Be (Refs. 20, 27, and 28) (open symbols, black and white).

We also examined the free-space atomic radii,<sup>29</sup> given in Table I, of the elements in these alloys to determine if there was any relation between the atomic radii and the spin-wave dispersion behavior. Although not seen in the Slater atomic radii,<sup>30</sup> also given in Table I, we see some correlation between the free-space atomic radii and the compositional behavior of the lattice parameters of the alloys. Al and Ga, whose alloys with Fe lie on the upper branch of Fig. 4, have atomic radii larger than that of  $\alpha$ -Fe. The free-space atomic radii of Ni, Co, and Si fall between 1.46 and 1.72 Å (as does  $\alpha$ -Fe), and their alloys with Fe are on the flat branch of lattice parameter versus concentration. Fe-Be values form the lower branch of the lattice parameter plot, and the atomic radius of Be is the smallest of the alloy constituents considered here. In spite of this observation, no correlation of the free-space atomic radii with  $D$  is observed.

TABLE I. Free-space atomic radii (Ref. 29), Slater (Ref. 30) atomic radii, and atomic weights for Fe and martensitic Fe-alloy constituents. Lines indicate breaks between the three different lattice constant behaviors discussed in the text.

Element	Atomic radius free space (Å)	Atomic radius Slater (Å)	Atomic weight (g/mole)
Al	1.82	1.25	26.9815
Ga	1.81	1.30	69.7230
Fe	1.72	1.40	55.8450
Ni	1.62	1.35	58.6934
Si	1.46	1.10	28.0855
Co	1.67	1.35	58.923
Be	1.40	1.05	9.0122

#### IV. CONCLUSIONS

We have measured the spin-wave dispersion relations for two dilute solid solution alloys of Fe with Ga,  $\text{Fe}_{1-x}\text{Ga}_x$ ,  $x = 0.160, 0.225$ , out to  $q \approx 0.8 \text{ \AA}^{-1}$  and energies up to 60 meV. No anomalous behavior attributable to the interaction between phonons and magnons was observed. The dispersion was found to be isotropic and adequately described in terms of the fourth-order expression in  $q$ . A correlation between the values of  $D$  obtained in this and in other works for other Fe alloys and the composition was observed. However, no correlation was indicated between the lattice parameter of the alloy and the free-space atomic radii of the solute and the values of  $D$ .

It is hoped that these and other similar data will motivate first-principles calculations of the ground-state spin dynam-

ics for these alloys. Such calculations may give the needed insight to the range of magnetic exchange and the observed isotropy of the spin-wave dispersion.

#### ACKNOWLEDGMENTS

This research was supported by the U.S. Department of Energy (DOE), Office of Basic Energy Sciences, Materials Sciences Division. The Ames Laboratory is operated by the Iowa State University for the U.S. DOE under Contract No. W-7405-ENG-82. We also acknowledge the support of the National Institute of Standards and Technology and the U.S. Department of Commerce in providing the neutron research facilities used in this work.

- 
- <sup>1</sup>*Etienne du Trémolet de Lacheisserie, Magnetostriction: Theory and Applications of Magnetoelasticity* (CRC Press, Boca Raton, FL, 1993).
- <sup>2</sup>*Handbook of Giant Magnetostrictive Materials*, edited by Göran Engdahl (Academic, New York, 2000).
- <sup>3</sup>Robert C. O'Handley, *Modern Magnetic Materials: Principles and Applications* (Wiley, New York, 2000).
- <sup>4</sup>M. Wuttig, L. Dai, and J. R. Cullen, *Appl. Phys. Lett.* **80**, 1135 (2002).
- <sup>5</sup>A. E. Clark, K. B. Hathaway, M. Wun-Fogle, J. B. Restorff, T. A. Lograsso, V. M. Keppens, G. Petculescu, and R. A. Taylor, *J. Appl. Phys.* **93**, 8621 (2003).
- <sup>6</sup>G. Petculescu, K. B. Hathaway, T. A. Lograsso, M. Wun-Fogle, and A. E. Clark, *J. Appl. Phys.* **97**, 10M315 (2005).
- <sup>7</sup>J. L. Zarestky, V. O. Garlea, T. A. Lograsso, D. L. Schlager, and C. Stassis, *Phys. Rev. B* **72**, 180408(R) (2005).
- <sup>8</sup>P. Zhao, J. Cullen, M. Wuttig, H. J. Kang, J. W. Lynn, T. A. Lograsso, and O. Moze, *J. Appl. Phys.* **99**, 08R101 (2006).
- <sup>9</sup>G. Shirane, V. J. Minkiewicz, and R. Nathans, *J. Appl. Phys.* **39**, 383 (1968).
- <sup>10</sup>M. F. Collins, V. J. Minkiewicz, R. Nathans, L. Passell, and G. Shirane, *Phys. Rev.* **179**, 417 (1969).
- <sup>11</sup>H. A. Mook and R. M. Nicklow, *Phys. Rev. B* **7**, 336 (1973).
- <sup>12</sup>J. W. Lynn, *Phys. Rev. B* **11**, 2624 (1975).
- <sup>13</sup>J. W. Lynn and H. A. Mook, *Physica B & C* **136**, 94 (1986).
- <sup>14</sup>B. Antonini and M. W. Stringfellow, *Proc. Phys. Soc. London* **89**, 419 (1966).
- <sup>15</sup>B. Antonini, F. Menzinger, A. Paoletti, and A. Tucciarone, *Phys. Rev.* **178**, 833 (1969).
- <sup>16</sup>M. Hatherly, K. Hirakawa, R. D. Lowde, J. F. Mallett, M. W. Stringfellow, and B. H. Torrie, *Proc. Phys. Soc. London* **84**, 55 (1964).
- <sup>17</sup>J. L. Zarestky (unpublished).
- <sup>18</sup>H. L. Luo, *Trans. Metall. Soc. AIME* **239**, 119 (1967).
- <sup>19</sup>R. A. Dunlap, J. D. McGraw, and S. P. Farrell, *J. Magn. Magn. Mater.* **305**, 315 (2006).
- <sup>20</sup>P. Mungsantisuk, R. P. Corson, and S. Guruswamy, *J. Appl. Phys.* **98**, 123907 (2005) and references therein.
- <sup>21</sup>M. Polcarová, K. Godwod, J. Bak-Misiuk, and S. Kadecvková, *Phys. Status Solidi A* **106**, 17 (1988).
- <sup>22</sup>G. H. Cockett and E. D. Davis, *J. Iron Steel Inst., London* **201**, 110 (1963).
- <sup>23</sup>M. C. Farquhar, H. Lipson, and A. R. Weill, *J. Iron Steel Inst., London* **152**, 457 (1945).
- <sup>24</sup>D. K. Chaudhuri, P. A. Ravindran, and J. J. Wert, *J. Appl. Phys.* **43**, 778 (1972).
- <sup>25</sup>R. P. Reed and R. E. Schramm, *J. Appl. Phys.* **40**, 3453 (1969).
- <sup>26</sup>H. Stuart and N. Ridley, *J. Appl. Phys., J. Phys. D* **2**, 485 (1969).
- <sup>27</sup>J. S. Gaev and R. S. Sokolov, *Metallurg.* **4**, 42 (1937).
- <sup>28</sup>O. Moze (unpublished).
- <sup>29</sup>C. F. Fischer, *At. Data* **4**, 301 (1972).
- <sup>30</sup>J. C. Slater, *J. Chem. Phys.* **41**, 3199 (1964).